Numerical solution of time fractional diffusion systems

Kevin Burrage[a,b,c], Angelamaria Cardone[d,*], Raffaele D'Ambrosio[d], Beatrice Paternoster[c]

[a]*Queensland University of Technology, Brisbane, Australia*
[b]*Department of Computer Science of Oxford University, Oxford OX13QD, UK*
[c]*ARC Centre of Excellence for Mathematical and Statistical Frontiers and School of Mathematical Sciences, Queensland University of Technology, Brisbane, Queensland 4000, Australia*
[d]*Dipartimento di Matematica, Università di Salerno, Via Giovanni Paolo II n. 132, I-84084 Fisciano (Salerno), Italy*

Abstract

In this paper a general class of diffusion problem is considered, where the standard time derivative is replaced by a fractional one. For the numerical solution, a mixed method is proposed, which consists of a finite difference scheme through space and a spectral collocation method through time. The spectral method considerably reduces the computational cost with respect to step-by-step methods to discretize the fractional derivative. Some classes of spectral bases are considered, which exhibit different convergence rates and some numerical results based on time diffusion reaction diffusion equations are given.

Keywords: diffusion systems, fractional differential equations, spectral methods, finite-difference schemes
2010 MSC: 35R11, 65M06, 65M70

1. Introduction

Although fractional calculus dates back to the XIX century, only in the last 50-60 years has growing interest been paid to this subject in modelling

*corresponding author
Email addresses: kevin.burrage@gmail.com (Kevin Burrage), ancardone@unisa.it (Angelamaria Cardone), rdambrosio@unisa.it (Raffaele D'Ambrosio), beapat@unisa.it (Beatrice Paternoster)

applications. The time fractional derivative ${}_0D_t^\alpha y(t)$ depends on the past history of the function $y(t)$, and so time fractional differential systems are naturally suitable to describe evolutionary processes with memory when $0 < \alpha \leq 1$. For values $1 < \alpha \leq 2$ the phenomena that are modelled have wave like properties - see [13]. Fractional models are increasingly used in many modelling situations including viscoelastic materials in mechanics [30, 42], anomalous diffusion in transport dynamics of complex systems [25, 33], soft tissues such as mitral valve in the human heart [40], some biological processes in rheology [12], the kinetics of complex systems in spatially crowded domains (compare [1] and references therein contained), the spread of HIV infection of CD4+ T-cells [11], Brownian motion [31, 34]. A number of applications modelled by time-fractional differential equations can be found in [21] and in the references therein. In many cases, the derivative index α belongs to the interval $(0, 1)$, like in [1, 11–13, 40, 41].

One important application area where both time and space fractional models are becoming important is in the field of water diffusion magnetic resonance imaging. Conventional MRI studies are based on the assumption of Gaussian diffusion, but biological tissues are structurally heterogeneous and under large diffusion weighting gradients the acquired signal has a heavy tail which is characteristic of anomalous diffusion [18] and hence fractional diffusion models are relevant. Anomalous diffusion MRI studies have been conducted in the brain [19], cardiac tissue [6], liver [3] and cartilage [37]. Specifically time fractional diffusion MRI models have been developed in [17, 29, 32], while fractional diffusion models of cardiac electrical propagation have been considered in [5, 8].

In this paper we consider a time-fractional reaction diffusion problem

$$\frac{\partial^\alpha u(x,t)}{\partial t^\alpha} = \frac{\partial^2}{\partial x^2} u(x,t) + f(t,x), \qquad (x,t) \in [0,X] \times [0,T], \tag{1.1}$$

subject to boundary conditions (such as Neumann or Dirichlet boundary conditions) as well as to suitable initial conditions. Here $u : [0,T] \times [0,X] \to \mathbb{R}$, $f : [0,T] \times [0,X] \to \mathbb{R}$. If $0 < \alpha \leq 1$ initial conditions are of the type $u(x,0) = u_0(x)$, if $1 < \alpha \leq 2$ initial conditions are of the type $u(x,0) = u_0(x)$, $u_t(x,0) = u_{t,0}(x)$ (compare [2, 21] and references therein). In the following we restrict our attention to the case $0 < \alpha < 1$. Some results of existence and uniqueness of solution can be found in [27, 28], where the analytical solution is also expressed in form of Fourier series. We adopt Caputo's definition of

fractional derivative:

$$\frac{\partial^\alpha y(t)}{\partial t^\alpha} = {}_0D_t^\alpha y(t) = \frac{1}{\Gamma(n-\alpha)} \int_0^t \frac{y^{(n)}(\tau)}{(t-\tau)^{\alpha+1-n}} d\tau, \quad n-1 < \alpha < n, \ n \in \mathbb{N}.$$

Some fundamental notions on fractional calculus may be found in [35].

One of the features of time fractional models is that they are examples of non-local models and as the solution depends on all its past history, numerical step-by-step methods are computationally expensive. On the other hand,it is well known that spectral methods can avoid the discretization of the 'heavy tail' and are exponentially convergent [23, 26, 41, 45, 46] and so are suitable for non-local problems avoiding the difficulty of using time discretization techniques that need to use all, or most, of the history. This motivates us to use a numerical scheme consisting of a spectral method through time, on a suitable basis of functions, and a finite-difference method through space, whose coefficients are adapted according to the qualitative behaviour of the solution.

The paper is organized as follows. In Section 2 we introduce a mixed spectral collocation method, applied to the semi-discrete problem generated by a finite difference scheme through space. Section 3 deals with the computation of matrix $\mathbf{D}$ and vector $\mathbf{d}$, which is a crucial part of the overall method. Section 4 is devoted to the choice of the bases of functions of the spectral method and of the collocation points. Some numerical experiments are illustrated in Section 5. Finally, we give some concluding remarks.

2. The method

We consider in a first analysis the time-fractional diffusion problem (1.1) subject to Neumann boundary conditions and initial conditions:

$$\frac{du(0,t)}{dx} = \frac{du(X,t)}{dx} = 0, t \in [0,T] \quad u(x,0) = u_0(x), x \in [0,X]. \tag{2.1}$$

2.1. Semi-discretization through space

The first step to solve the problem (1.1)(2.1) consists of applying a finite-difference scheme to discretize the spatial derivative. We use a space discretization which is suitable to treat both Neumann and Dirichlet condition. We introduce a uniform mesh on $[0, X]$, given by:

$$x_0 = 0 < x_1 < \cdots < x_M, \quad x_m = m\Delta x, \quad \Delta x = X/M.$$

To approximate the spatial derivative in (1.1), in the internal points, we adopt this centered finite difference scheme:

$$\frac{\partial^2 u(x_i,t)}{\partial x^2} = \frac{a_2 u(x_{i-1},t) + a_1 u(x_i,t) + a_0 u(x_{i+1},t)}{(\Delta x)^2} + \frac{\partial^4 u(\xi,t)}{\partial x^4}\frac{(\Delta x)^2}{12}, \quad (2.2)$$

$\xi \in [x_{i-1}, x_{i+1}]$, assuming that u is sufficiently smooth.
In the case of the classical centered finite difference scheme, we have $a_0 = a_2 = -1$ and $a_1 = 2$. Alternatively, if the solution has an oscillatory behavior with respect to the spatial variable, and an estimate of the frequency is available, we may apply the exponentially-fitted centered finite difference scheme introduced in [9, 10] (compare also [7]). We refer to [9] for the exact expression of coefficients a_0, a_1 and a_2 in this case. An extensive monograph on the exponential fitting theory is [20].
At the boundary, we consider two different second order approximations of the Neumann condition: the centered difference approximation

$$u_x(x,t) = \frac{u(x+\Delta x,t) - u(x-\Delta x,t)}{2\Delta x} + \frac{(\Delta x)^2}{6}u_{xx}(x,t) + O((\Delta x)^4) \quad (2.3)$$

and

$$\begin{aligned} u_x(x_0,t) = \quad & \frac{-3u(x_0,t) + 4u(x_0+\Delta x,t) - u(x_0+2\Delta x,t)}{2\Delta x} \\ & + \tfrac{(\Delta x)^2}{3}u_{xx}(x_0,t) + O((\Delta x)^3), \\ u_x(x_M,t) = \quad & \frac{-3u(x_M,t) + 4u(x-\Delta x,t) - u(x_M-2\Delta x,t)}{-2\Delta x} \\ & + \tfrac{(\Delta x)^2}{3}u_{xx}(x_M,t) + O((\Delta x)^3). \end{aligned} \quad (2.4)$$

Placing the nodes on the vertex of each cell gives rise to a common space discretization to treat both Neumann and Dirichlet conditions. Moreover, this choice is totally in line with the existing literature regarding the method of lines [38, 39], also in its adapted version with non-polynomial basis [7, 9, 10].

By introducing the discrete differential operator L:

$$Lu(x_i,t) = \frac{a_2 u(x_{i-1},t) + a_1 u(x_i,t) + a_0 u(x_{i+1},t)}{(\Delta x)^2},$$

at the internal mesh points, the equation (1.1) may be written as

$$\frac{\partial^\alpha u(x_i,t)}{\partial t^\alpha} = Lu(x_i,t) + f(x_i,t) + R(x_i,t), \quad i = 1,\dots,M-1,$$

where

$$|R(x_i,t)| \leq \frac{1}{12} \max_{[0,X]\times[0,T]} \left| \frac{\partial^4}{\partial x^4} u(x,t) \right| (\Delta x)^2. \tag{2.5}$$

Then, the semi-discretization of (1.1) is given by

$$\frac{\partial^\alpha \mathbf{u}(t)}{\partial t^\alpha} = \mathbf{L}\mathbf{u}(t) + \mathbf{f}(t), \tag{2.6}$$

where $\mathbf{u}(t) = [u^1(t) \dots u^{M-1}(t)]^T$, $u^i(t)$ is an approximation of $u(x_i,t)$, $\mathbf{f}(t) = [f(x_1,t) \dots f(x_{M-1},t)]^T$, $\mathbf{L}$ is the following tridiagonal matrix of dimension $M-1$:

$$\mathbf{L} = \begin{bmatrix} a_1 & a_0 & & & & & \\ a_2 & a_1 & a_0 & & & & \\ & \ddots & \ddots & \ddots & & & \\ & & & a_2 & a_1 & a_0 & \\ & & & & a_2 & a_1 & \end{bmatrix}. \tag{2.7}$$

If the boundary conditions are discretized by (2.3), we have:

$$u^{-1}(t) = u^1(t) \quad \text{and} \quad u^{M+1}(t) = u^{M-1}(t), \tag{2.8}$$

while if we apply (2.4), it gives

$$u^0(t) = \frac{4}{3}u^1(t) - \frac{1}{3}u^2(t) \quad \text{and} \quad u^M(t) = \frac{4}{3}u^{M-1}(t) - \frac{1}{3}u^{M-2}(t). \tag{2.9}$$

Both schemes (2.2)(2.8) and (2.2)(2.9) are second order accurate, thanks to (2.3)-(2.5).

2.2. Full discretization

We approximate each component $u^i(t)$ of the solution of (2.6) by a function $u_N^i(t)$ of the type

$$u_N^i(t) = \sum_{j=0}^{N} \hat{u}_j^i \mathcal{P}_j(t) \qquad \text{(modal expansion)}. \tag{2.10}$$

By introducing a set of collocation points $t_0 = 0 < t_1 < \dots < t_N = T$, this approximation can be also expressed as

$$u_N^i(t) = \sum_{j=0}^{N} \varphi_j(t) u_N^i(t_j) \qquad \text{(nodal expansion)}. \tag{2.11}$$

The above functions $\mathcal{P}_j(t)$ are chosen both to well reproduce the behavior of the analytical solution, and such that their fractional derivative can be easily computed analytically. The choice of the basis functions $\mathcal{P}_j(t)$, $j = 0, \ldots, N$, will be discussed in Sec. 4. On the other hand, functions $\varphi_j(t)$ (and their fractional derivatives) are not known and should be computed in some way. We observe that from (2.11) they have to satisfy $\varphi_j(t_k) = \delta_{j,k}$, where $\delta_{j,k}$ is the Kronecker delta. We define

$$\psi_j(t) := {}_0D_t^\alpha \varphi_j(t),$$

then we derive the following approximation

$${}_0D_t^\alpha u^i(t) \approx {}_0D_t^\alpha u_N^i(t) = \sum_{j=0}^{N} \psi_j(t) u_N^i(t_j).$$

Therefore we impose

$${}_0D_t^\alpha u^i(t_k) \approx \sum_{j=0}^{N} \psi_j(t_k) u_{i,j} = \sum_{j=1}^{N} \psi_j(t_k) u_{i,j} + \psi_0(t_k) u_0(x_i), \tag{2.12}$$

$k = 1, \ldots, N$, where $u_{i,j} = u_N^i(t_j) \approx u(x_i, t_j)$ and $u_0(x)$ is given by (2.1). In equation (2.6), we substitute the fractional derivative of $u^i(t)$ in $t = t_k$ by (2.12) and, by adding the discretized boundary conditions, we obtain a system of $N(M+1)$ equations in $N(M+1)$ unknowns $u_{i,j}$, $i = 0, \ldots, M$, $k = 1, \ldots, N$. As a matter of fact, once the basis of functions $\{\mathcal{P}_j(t)\}_{j=0}^N$ is chosen, the values $\psi_j(t_k)$, $j = 0, \ldots, N$, $k = 1, \ldots, N$ can be easily computed, as it will be shown in Sec. 3. In the following subsections we will examine in some details the fully discrete systems corresponding to the various discretized boundary conditions.

2.2.1. Boundary conditions discretized by centered difference (2.3)

By discretizing the boundary conditions with formula (2.3), we get (2.8) and, by (2.6), we obtain

$$\begin{aligned}
\sum_{j=0}^{N} \psi_j(t_k) u_{0,j} &= \frac{(a_0+a_2)u_{1,k} + a_1 u_{0,k}}{(\Delta x)^2} + f(x_0, t_k), \\
\sum_{j=0}^{N} \psi_j(t_k) u_{i,j} &= \frac{a_2 u_{i-1,k} + a_1 u_{i,k} + a_0 u_{i+1,k}}{(\Delta x)^2} + f(x_i, t_k), i = 1, \ldots, M-1, \\
\sum_{j=0}^{N} \psi_j(t_k) u_{M,j} &= \frac{(a_0+a_2)u_{M-1,k} + a_1 u_{M,k}}{(\Delta x)^2} + f(x_M, t_k),
\end{aligned}$$

with $k = 1, ..., N$. Hence, the fully discretized counterpart of the problem (1.1)(2.1) is given by the following linear system

$$\mathbf{D}\mathbf{U} + \mathbf{d}\,\mathbf{u_0}^T = \frac{1}{\Delta x^2}\mathbf{U}\mathbf{M} + \mathbf{F}. \tag{2.13}$$

The square matrix $\mathbf{M}$, of dimension $(M+1)$, is defined as

$$\mathbf{M} = \begin{bmatrix}
a_1 & a_2 & & & & & \\
(a_0+a_2) & a_1 & a_2 & & & & \\
 & a_0 & a_1 & a_2 & & & \\
 & & \ddots & \ddots & \ddots & & \\
 & & & a_0 & a_1 & a_2 & \\
 & & & & a_0 & a_1 & (a_0+a_2) \\
 & & & & & a_0 & a_1
\end{bmatrix}.$$

Moreover

$$(\mathbf{D})_{k,j} = \psi_j(t_k),\ (\mathbf{d})_k = \psi_0(t_k),\ k, j = 1, \ldots, N, \tag{2.14}$$

and

$$(\mathbf{u_0})_{i+1} = u_0(x_i),\ (\mathbf{U})_{k,i+1} = u_{i,k},\ (\mathbf{F})_{k,i+1} = f(x_i, t_k),$$

$k = 1, \ldots, N, i = 0, \ldots, M$. Matrix $\mathbf{D}$ and vector $\mathbf{d}$ will be computed in Sec. 3. Equation (2.13) is a Sylvester equation, whose solution is unique if and only if the matrices $(\Delta x)^2\mathbf{D}$ and $\mathbf{M}$ have distinct eigenvalues [4].

2.2.2. Boundary conditions discretized by (2.4)

From the approximation (2.4) at the boundary nodes, we obtain (2.9), thus we get $u_{0,k} = \frac{4}{3}u_{1,k} - \frac{1}{3}u_{2,k}$ and $u_{M,k} = \frac{4}{3}u_{M-1,k} - \frac{1}{3}u_{M-2,k}$. Likewise the previous case, we formulate a Sylvester equation of type (2.13), where the square matrix $\mathbf{M}$ has dimension $(M-1)$ and is defined as

$$\mathbf{M} = \begin{bmatrix} (a_1 + \frac{4}{3}a_2) & a_2 & & & & & & \\ (a_0 - \frac{1}{3}a_2) & a_1 & a_2 & & & & & \\ & a_0 & a_1 & a_2 & & & & \\ & & \ddots & \ddots & \ddots & & & \\ & & & a_0 & a_1 & a_2 & & \\ & & & & a_0 & a_1 & (a_2 - \frac{1}{3}a_0) & \\ & & & & & a_0 & (a_1 + \frac{4}{3}a_0) \end{bmatrix},$$

the matrix $\mathbf{D}$ and the vector $\mathbf{d}$ are given in (2.14) and

$$(\mathbf{U})_{k,i} = u_{i,k}, (\mathbf{F})_{k,i} = f(x_i, t_k), (\mathbf{u_0})_i = u_0(x_i), \tag{2.15}$$

$k = 1, \ldots, N$, $i = 1, \ldots, M-1$.

2.3. Problem (1.1) *with Dirichlet conditions*

Now we consider the problem (1.1) with the homogeneous Dirichlet conditions and initial value $u_0(x)$:

$$u(0,t) = u(X,t) = 0, t \in [0,T] \quad u(x,0) = u_0(x), x \in [0,X]. \tag{2.16}$$

By the same centered finite difference scheme (2.2), we obtain the semi-discrete system (2.6) with $u^0(t) = u^M(t) = 0$. Then, by applying the spectral-collocation method we get the fully discrete system with the additional conditions $u_{0,k} = 0$, and $u_{M,k} = 0$, $k = 1, ..., N$. This system is equivalent to a Sylvester equation of type (2.13), with $\mathbf{M} = \mathbf{L}^T$, where $\mathbf{L}$ is defined in (2.7). The other matrices and vectors are defined as in (2.15).

3. Computation of matrix D and vector d

To formulate the discrete system (2.13) we have to compute matrix $\mathbf{D}$ and vector $\mathbf{d}$, whose entries are given by the evaluation of functions $\psi_j(t) = {}_0D_t^{\alpha}\varphi_j(t)$ at the collocation points t_k. Functions $\varphi_j(t)$ may be analytically

computed by (2.10) and (2.11), and then $\psi_j(t)$ are derived. In practice, this analytical approach is highly time-consuming even by using some symbolic tools (such as Mathematica®) and not applicable at all for $N > 4$. Moreover, such procedure is not portable in a routine for the solution of the problem (1.1)(2.1). Thus, it is necessary to find an automatic procedure, which does not involve any symbolic calculation. This goal may be achieved by virtue of the following proposition. Here we adopt Matlab notation and $[\mathbf{d}, \mathbf{D}]$ is the matrix whose first column is vector $\mathbf{d}$ and the other columns are given by matrix $\mathbf{D}$.

Proposition 3.1. *The following equality holds:*

$$[\mathbf{d}, \mathbf{D}] = \mathcal{P} \cdot \mathbf{B}, \tag{3.1}$$

where $\mathbf{B} = \mathbf{A}^{-1}$ *and*

$$\mathbf{A} = \begin{bmatrix} \mathcal{P}_0(t_0) & \cdots & \mathcal{P}_N(t_0) \\ \vdots & \ddots & \vdots \\ \mathcal{P}_0(t_N) & \cdots & \mathcal{P}_N(t_N) \end{bmatrix}, \mathcal{P} = \begin{bmatrix} D^\alpha \mathcal{P}_0(t_1) & \cdots & D^\alpha \mathcal{P}_N(t_1) \\ \vdots & \ddots & \vdots \\ D^\alpha \mathcal{P}_0(t_N) & \cdots & D^\alpha \mathcal{P}_N(t_N) \end{bmatrix}.$$

Proof. By applying the interpolation conditions at the points $t_0, t_1, \ldots, t_N$, to the modal expansion (2.10), we get the linear system of dimension $N+1$

$$A\hat{\mathbf{u}}^i = \mathbf{u}_N^i,$$

where $\hat{\mathbf{u}}^i = \begin{bmatrix} \hat{u}_0^i & \ldots & \hat{u}_N^i \end{bmatrix}^T$, $\mathbf{u_N}^i = \begin{bmatrix} u_N^i(t_0) & \ldots & u_N^i(t_N) \end{bmatrix}^T$. Thus

$$\hat{\mathbf{u}}^i = A^{-1}\mathbf{u}_N^i = \mathbf{B}\mathbf{u}_N^i, \quad \text{i.e.} \quad \hat{u}_l^i = \sum_{j=0}^{N} \mathbf{B}_{lj} u_N^i(t_j), l = 0, \ldots, N.$$

Then

$$u_N^i(t) = \sum_{l=0}^{N} \hat{u}_l^i \mathcal{P}_l(t) = \sum_{l=0}^{N} \mathcal{P}_l(t) \sum_{j=0}^{N} \mathbf{B}_{lj} u_N^i(t_j) = \sum_{j=0}^{N} \left(\sum_{l=0}^{N} \mathbf{B}_{lj} \mathcal{P}_l(t) \right) u_N^i(t_j).$$

From this we obtain the functions $\varphi_j(t)$ of the nodal expansion (2.11) and their fractional derivatives:

$$\varphi_j(t) = \sum_{l=0}^{N} \mathbf{B}_{lj} P_l(t), \qquad \psi_j(t) := {}_0D_t^\alpha \varphi_j(t) = \sum_{l=0}^{N} \mathbf{B}_{lj} \, {}_0D_t^\alpha \mathcal{P}_l(t),$$

and (3.1) follows. □

We notice that the computation of $\mathbf{A}^{-1}$ is not expensive, since N usually is small ($N < 10$, as we will see in the numerical experiments), although the condition number of $\mathbf{A}$ may affect the accuracy.

The computational kernel of the proposed method consists of the computation of matrix $\mathbf{D}$, and of the solution of the Sylvester equation (2.13). Thanks to Prop. 3.1, the construction of $\mathbf{D}$ requires the inversion of a matrix of dimension N and a matrix multiplication, therefore the computational cost is $O(N^4)$. The solution of the Sylvester system (2.13) is a matrix of dimension less or equal to NM, thus by a direct solver method the computational cost is $O(NM)^3$, but this cost may be reduced to $O(N^3 + M^3)$ [4].

4. Function bases and collocation points of the spectral method

We consider three different classes of functions as basis for the spectral method: a power basis, a polynomial basis and a trigonometric basis. Each of them satisfies the condition to have a fractional derivative defined in $\mathbb{R}$.

In the case of (1.1) with $f = 0$ and when the Laplacian is replaced by the discrete operator A, the solution of the ensuing linear systems is given by

$$y(t) = E_\alpha(At^\alpha)y_0.$$

Here

$$E_\alpha(z) = \sum_{j=0}^{\infty} \frac{z^j}{\Gamma(1+\alpha j)}$$

is the Mittag Leffler (ML) function and Γ is the gamma function, see the monograph [24] and survey [16] on the properties of generalised ML functions. Note $E_1(z) = \exp(z)$ and a characteristic of ML functions is a heavy tail. As the general solution of the test problem (1.1)(2.1) depends on the ML function, one natural choice for the function basis $\{\varphi_j\}_{j=0}^N$ is:

$$1, t^\alpha, t^{2\alpha}, \ldots, t^{N\alpha}, \tag{4.1}$$

The fractional derivatives of such functions are given by (compare e.g. [35])

$${}_0D_t^\alpha\ 1 = 0, \qquad {}_0D_t^\alpha\ t^{j\alpha} = \frac{\Gamma(\alpha j + 1)}{\Gamma(\alpha(j-1)+1)} t^{\alpha(j-1)}, \quad j = 1, 2, \ldots.$$

A second basis consists of a class of Jacobi polynomials shifted in the interval $[0, T]$. We recall that Jacobi polynomials $P_n^{(a,b)}(x)$ are orthogonal

with respect to the weight function $(1-x)^a(1+x)^b$ in the interval $[-1,1]$. The n-th Jacobi polynomial shifted in $[0,T]$ is $P_{n,T}^{(a,b)}(x) = P_n^{(a,b)}(\frac{2x}{T}-1)$. We adopt the class of Jacobi polynomials $P_n^{(0,-\nu)}(x)$ shifted in $[0,T]$, with $\nu = \lceil \alpha \rceil$. The choice of this basis is inspired by the spectral theory developed for the fractional Sturm Liouville problem in [43] (see also [46]). If $0 < \alpha \leq 1$, we have

$$P_{n,T}^{(0,1)}(x) = \sum_{k=0}^{n} (-1)^{n-k} \frac{(n+k+1)!}{(k+1)!(n-k)!k!T^k} x^k. \tag{4.2}$$

Its fractional derivative is easy to compute, and for $k \in \mathbb{N}$ gives

$${}_0D_x^\alpha x^k = \begin{cases} \frac{k!}{\Gamma(k-\alpha+1)} x^{k-\alpha}, & \text{if } k \geq \lceil \alpha \rceil, \\ 0, & \text{otherwise.} \end{cases}$$

Another possible choice, which may be useful for oscillatory problems, is the trigonometric basis

$$1, \cos(\omega t), \sin \omega t, \cos(2\omega t), \sin(2\omega t), \ldots, \cos\left(\frac{N}{2}\omega t\right), \sin\left(\frac{N}{2}\omega t\right), \tag{4.3}$$

where N is even and ω is an estimate of the frequency of the solution. In this case, the fractional derivatives are also easy to compute and

$${}_0D_t^\alpha \cos(j\omega t) = (\omega j)^\alpha \cos\left(\omega j t + \alpha\frac{\pi}{2}\right), \quad {}_0D_t^\alpha \sin(j\omega t) = (\omega j)^\alpha \sin\left(\omega j t + \alpha\frac{\pi}{2}\right).$$

We note that the behaviour of the error is affected not only by the choice of a suitable basis of functions, but also by the choice of the collocation points. The easiest choice is to consider equidistant nodes in the time interval $[0,T]$. We consider Chebyshev zeros and extrema shifted in $[0,T]$, since the properties of these points in the interpolation theory may help to reduce the collocation error.

5. Numerical experiments

We performed the numerical tests in Matlab. To solve the full-discrete Sylvester system (2.13) we applied the Matlab function lyap. In the following tables and figures we report the error computed in l_∞-norm

$$error := \max_{0\leq i\leq M} \max_{1\leq k\leq N} |u_{ik} - u(x_i, t_k)|,$$

where $u(x,t)$ is the exact solution of the considered problem.

5.1. Test example 1

We consider as a test example the time-fractional heat equation, i.e. the problem (1.1)(2.1) with $f(x,t) = 0$. If $u_0(x)$ and $u_0'(x)$ are piecewise continuous in $[0, X]$, the general solution is [22]

$$u(x,t) = \frac{c_0}{2} + \sum_{k=1}^{\infty} c_k \cos\left(\frac{k\pi x}{X}\right) E_\alpha(-(k\pi/X)^2 t^\alpha),$$

and

$$c_k = \frac{2}{X}\int_0^X u_0(s)\cos\left(\frac{k\pi s}{X}\right) ds, \quad k \geq 0.$$

If we consider

$$X = 2\pi, u_0(x) = -0.05\cos(x), \tag{5.1}$$

we get by simple calculations $u(x,t) = -0.05\cos(x)E_\alpha(-t^\alpha)$.
To evaluate the exact solution, we computed the ML function by Matlab codes mlf [36] and ml [14, 15], which have the same accuracy but the latter is much faster.

In order to numerically verify the accuracy of the space-discretization, we fix a sufficiently large number N of the functions of the spectral basis and vary the dimension of the space mesh M. In this way that the error due to the spectral method along time is negligible and the global error is essentially given by the spatial discretization. The results are listed in Tab. 1, where cd indicates the number of correct digits of the solution (the error is written as 10^{-cd}) and the effective order is computed by the following formula

$$p_{eff} = \frac{cd(M) - cd(M/2)}{\log_{10} 2}.$$

The effective order of classical finite difference is 2, both in the case of the scheme class1 described in Subsubsec. 2.2.1 and in the case of class2, described in Subsubsec. 2.2.2. On the other hand, the exponentially-fitted finite difference [9] has effective order equal to 3: we suppose that the first term of the error expansion vanishes thanks to the special form of the exact solution and to the fact that the coefficients a_0, a_1, a_2 depends on the frequency of the solution. We obtained similar results with other values of α.

Now we analyze the error due to the spectral method through time. To this aim, we fix a large value M of the space mesh and let N vary, i.e. the

Table 1: Error on test example 1, $\alpha = 1/2$ and $T = 1$. Power basis (4.1) through time with equidistant collocation points.

	class1 $N = 9$		class2 $N = 9$		exp-fitt $N = 8$	
M	cd	p_{eff}	cd	p_{eff}	cd	p_{eff}
5	2.73		1.86		1.82	
10	3.34	2.01	2.88	3.40	2.77	3.14
20	3.94	2.00	3.88	3.30	3.68	3.05
40	4.54	2.00	4.51	1.12	4.59	3.01
80	5.14	2.00	5.13	2.06	5.50	3.01
160	5.74	2.00	5.75	2.04	6.41	3.04

dimension of the spectral basis. Since the accuracy of the overall scheme depends both on the discretization error and on the accuracy of the solution of the system (2.13), we analyzed the condition number of matrix $\mathbf{D}$ too. In Fig. 1 we plotted the error and the condition number of $\mathbf{D}$ for the power spectral basis (4.1). For $\alpha = 1/2$ the method exhibits an exponential convergence, while the condition number of $\mathbf{D}$ is increasing with N. The ill-conditioning of $\mathbf{D}$ is responsible for the loss of accuracy for $N > 9$. A similar behavior is observed for $\alpha = 1/10$, where the condition number of $\mathbf{D}$ grows faster. We notice that in both cases, the exponential convergence is lost as $cond(\mathbf{D}) > 10^6$. No significant difference is shown by varying the set of collocation points. For $\alpha = 9/10$, $cond(\mathbf{D})$ is much smaller, especially for the Chebyshev roots and extrema, and consequently the accuracy of the method is preserved. The reason for a flat line of the error for $N > 8$ is that the error of the space-discretization has become predominant with respect to the error through time.

In Fig. 2 some experiments with the Jacobi polynomials (4.2) are shown. The convergence rate is considerably slower with respect to the power basis, and poor results are observed for $\alpha = 1/10$. Thus, the Jacobi polynomial basis proves not to be suitable to approximate the considered problems because, we assume, it does not reflect the behavior of the analytical solution. This is in agreement with [44], where the convergence is slower if the solution is not sufficiently smooth. Finally, we performed some tests with the trigonometric basis (4.3), but no convergence is seen, and moreover matrix $\mathbf{D}$ is badly conditioned even for small values of N. In Fig. 2 the case $\alpha = 1/2$

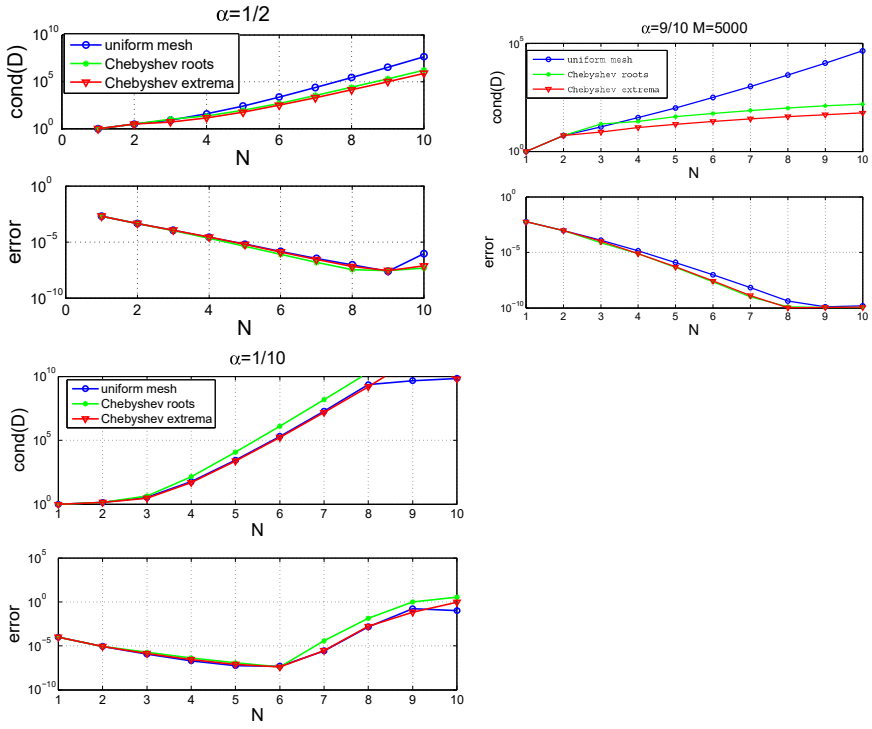

Figure 1: Test example 1, $T = 1$. Condition number of matrix D and error with spectral method by power basis (4.1) through time, and classical finite differences through space. $M = 1250$ except for $\alpha = 9/10$. There is a logarithmic scale on the y-axis.

and $\omega = 1$ is shown, but similar results are obtained for other values of α and ω. These results do not surprise, since the problem is not oscillatory in time.

To analyze the performances of the spectral method for a larger time-integration interval we set $T = 10$ and we carried out some tests for $\alpha = 1/2$. The results are plotted in Fig. 3. The performances are analogous to the case $T = 1$, although the convergence is somewhat slower.

5.2. Test example 2

Now we consider as test example the problem (1.1)(2.16) with $f(x, t) = 0$. If $u_0(x)$ and $u_0'(x)$ are piecewise continuous in $[0, X]$, the general solution is [2]

$$u(x,t) = \sum_{k=0}^{\infty} c_k \sin\left(\frac{k\pi x}{X}\right) E_\alpha(-(k\pi/X)^2 t^\alpha),$$

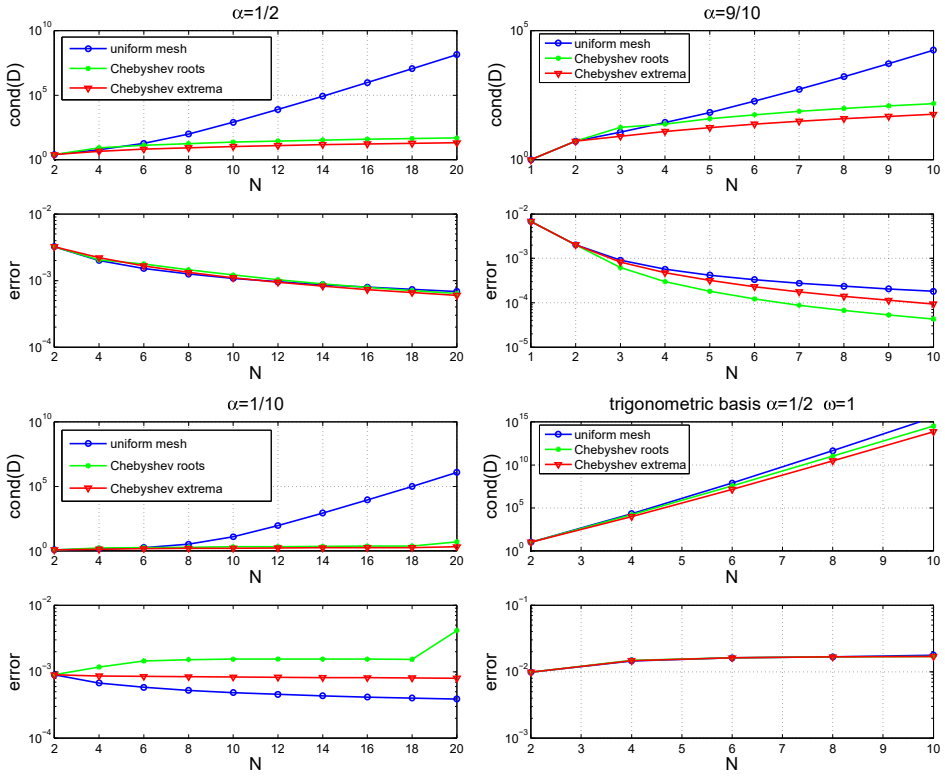

Figure 2: Test example 1, $T = 1$. Condition number of matrix D and error by Jacobi polynomials (4.2) (up and bottom left) and by trigonometric basis (4.3) (bottom, right). $M = 1250$. There is a logarithmic scale on the y-axis.

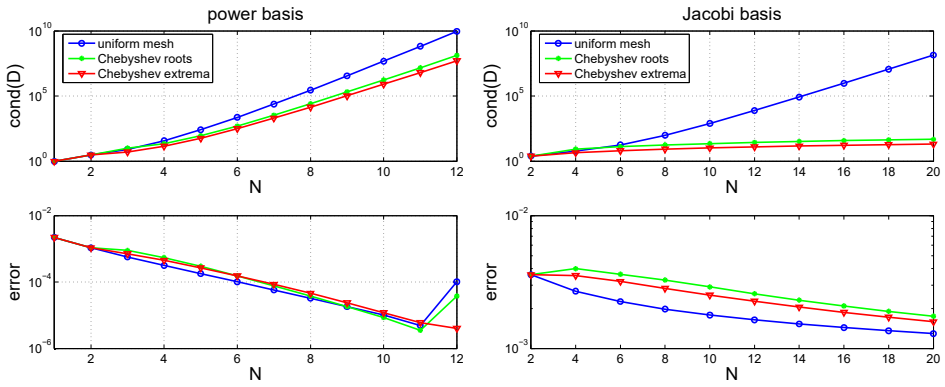

Figure 3: Test example 1, $\alpha = 1/2$, $T = 10$. Condition number of matrix D and error by power basis (4.1) (left) and Jacobi polynomials (4.2) (right). $M = 1250$. There is a logarithmic scale on the y-axis.

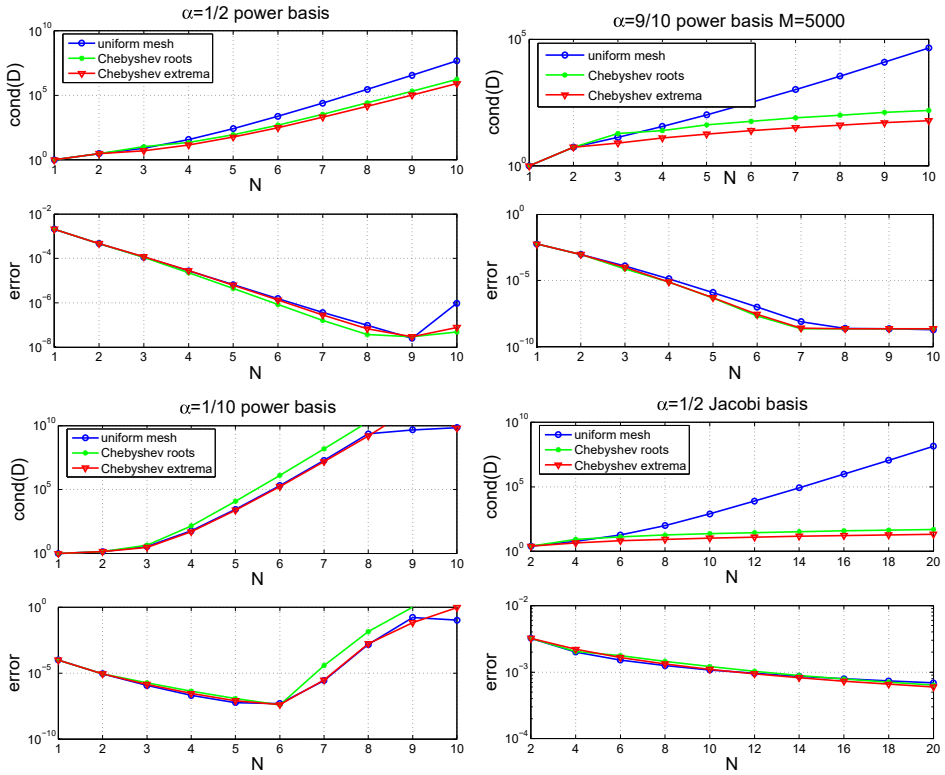

Figure 4: Test example 2, $T = 1$. Condition number of matrix D and error by power basis (4.1), except for bottom, right, where the Jacobi basis (4.2) was applied. $M = 1250$ where not otherwise specified. There is a logarithmic scale on the y-axis.

and

$$c_k = \frac{2}{X}\int_0^X u_0(s)\sin\left(\frac{k\pi s}{X}\right)ds, \quad k \geq 0.$$

If we consider

$$X = 2\pi, u_0(x) = -0.05\sin(x), \tag{5.2}$$

we get by simple calculations $u(x,t) = -0.05\sin(x)E_\alpha(-t^\alpha)$.
In Fig. 4 and 5 some numerical experiments are shown. The performances of the method are completely analogous to the case of Neumann conditions.

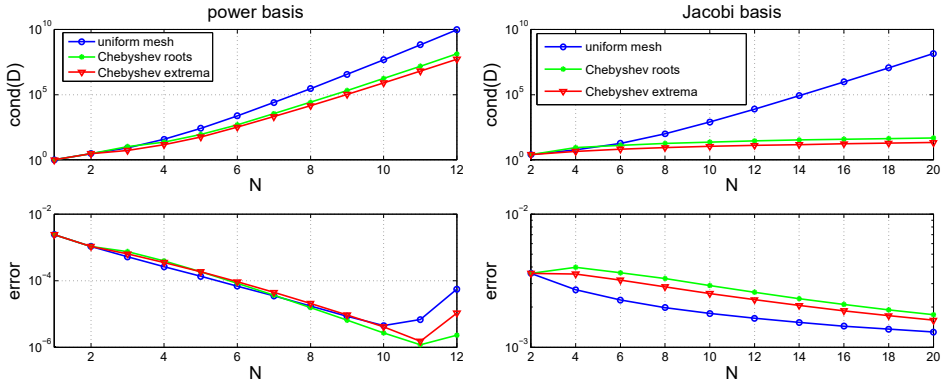

Figure 5: Test example 2, $\alpha = 1/2$, $T = 10$. Condition number of matrix D and error by power basis (4.1) (left) and Jacobi basis (4.2) (right). $M = 1250$. There is a logarithmic scale on the y-axis.

5.3. Test example 3

Last test example is a nonlinear problem, i.e. a problem where the forcing function depends on x, t and u. In particular, we consider the problem

$$\frac{\partial^\alpha u(x,t)}{\partial t^\alpha} = \frac{\partial^2}{\partial x^2} u(x,t) + u - \frac{u^3}{3} + g(x,t), \qquad (x,t) \in [0,1] \times [0,1], \quad (5.3)$$

subject to Neumann boundary conditions and with initial condition $u_0(x) = 0$. The function $g(x,t)$ is such that $u(x,t) = x^2(3-2x)t^{3+\alpha}$. This type of equation has been proposed in [13], where a two-dimensional problem is considered, with the same type of nonlinearity.

By applying our method to problem (5.3) we obtain system (2.13), where the matrix $\mathbf{F}$ now depends on $\mathbf{U}$, thus we have to solve a nonlinear system of dimension $N(M-1)$. We used Matlab function fsolve, with starting guess given by the null solution, with tolerance required for the function value equal to 10^{-14}. The results of numerical experiments are illustrated in Fig. 6, where we set $\alpha = 0.8$, as done in [13]. We observe exponential convergence both in the case of power basis (4.1) and of Jacobi basis (4.2). As a matter of fact, as N increases the error of the spectral method vanishes and the global error is given by the error of the finite difference method along space.

5.4. Test example 4

Finally we apply our method to equation (5.3) with $\alpha = 0.8$, $g(x,t) = 0$ and $u_0(x) = \bar{n}_1 - 0.05\cos(k_0 x)$, with $\bar{n}_1 = 0.099669956223526$ and $k_0 =$

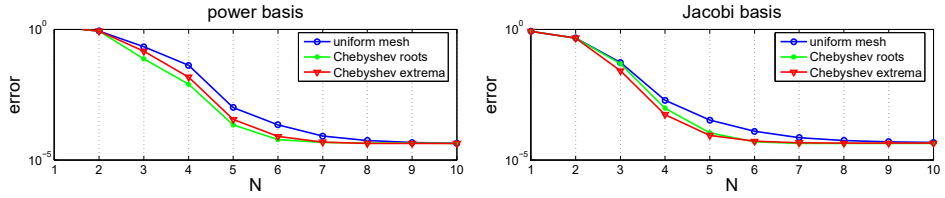

Figure 6: Test example 3, $\alpha = 0.8$. Error by power basis (4.1) (left) and by Jacobi basis (4.2) (right). $M = 200$. There is a logarithmic scale on the y-axis.

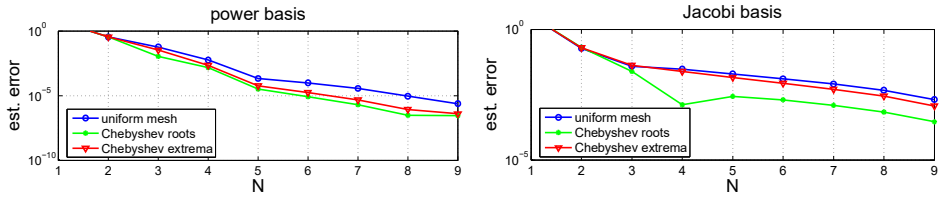

Figure 7: Test example 4, $\alpha = 0.8$. Estimated error by power basis (4.1) (left) and Jacobi basis (4.2) (right). $M = 200$. There is a logarithmic scale on the y-axis.

0.474040841239853. These parameters are taken from [13]. The analytical solution of this problem is not known. Thus, to verify the convergence, we set as reference solution the numerical solution obtained with 10 functions of the spectral basis. Then we compute the estimated error as the l_2-norm of the difference between the solution with N functions and the reference solution, computed at the last time step. The results are illustrated in Fig. 7. We observe that also in this case the spectral method exhibits exponential convergence, and the best rate of convergence is obtained with power basis.

6. Conclusions

We introduced a mixed spectral method to solve a time-fractional diffusion problem. It consists of a finite difference through space, where the coefficients may depend on an estimate of the frequency in the case of periodic problems, and of a spectral collocation method through time on a suitable function basis. We underline that any symbolic computation has been avoided and the method can be implemented straightforwardly in an algorithm. The numerical experiments confirmed the order of accuracy of the spatial discretization and showed that, if the spectral basis is suitably chosen, the spectral method exhibits an exponential convergence.

Acknowledgements. A. Cardone, R. D'Ambrosio and B. Paternoster were supported by GNCS-INdAM. Authors wish to express their gratitude to the anonymous referees for their helpful observations.

References

[1] F. Abdullah, Using fractional differential equations to model the Michaelis-Menten reaction in a 2-d region containing obstacles, ScienceAsia 37 (2011) 75–78.

[2] O.P. Agrawal, Solution for a fractional diffusion-wave equation defined in a bounded domain, Nonlinear Dynam. 29 (2002) 145–155. Fractional order calculus and its applications.

[3] S. Anderson, B. Barry, J. Soto, A. Ozonoff, M. O'Brien, H. Jara, Characterizing non-Gaussian, high b-value diffusion in liver fibrosis: Stretched exponential and diffusional kurtosis modeling, J. Magn. Reson. Imaging 39 (2014) 827–834.

[4] R.H. Bartels, G.W. Stewart, Solution of the matrix equation $AX + XB = C$ [F4], Commun. ACM 15 (1972) 820–826.

[5] A. Bueno-Orovio, D. Kay, V. Grau, B. Rodriguez, K. Burrage, Fractional diffusion models of cardiac electrical propagation: Role of structural heterogeneity in dispersion of repolarization, J. R. Soc. Interface 11 (2014).

[6] A. Bueno-Orovio, I. Teh, J. Schneider, K. Burrage, V. Grau, Anomalous diffusion in cardiac tissue as an index of myocardial microstructure, IEEE Trans. Med. Imaging 35 (2016) 2200–2207.

[7] A. Cardone, R. D'Ambrosio, B. Paternoster, Exponentially fitted IMEX methods for advection–diffusion problems, J. Comput. Appl. Math. 316 (2017) 100–108.

[8] N. Cusimano, A. Bueno-Orovio, I. Turner, K. Burrage, On the order of the fractional laplacian in determining the spatio-temporal evolution of a space-fractional model of cardiac electrophysiology, PLoS ONE 10 (2015).

[9] R. D'Ambrosio, B. Paternoster, Numerical solution of a diffusion problem by exponentially fitted finite difference methods, SpringerPlus 3 (2014) 425.

[10] R. D'Ambrosio, B. Paternoster, Numerical solution of reaction–diffusion systems of λ–ω type by trigonometrically fitted methods, J. Comput. Appl. Math. 294 (2016) 436–445.

[11] Y. Ding, H. Ye, A fractional-order differential equation model of HIV infection of $CD4^+$ T-cells, Math. Comput. Modelling 50 (2009) 386–392.

[12] V. Djordjević, J. Jarić, B. Fabry, J. Fredberg, D. Stamenović, Fractional derivatives embody essential features of cell rheological behavior, Ann. Biomed. Eng. 31 (2003) 692–699.

[13] V. Gafiychuk, B. Datsko, V. Meleshko, Mathematical modeling of time fractional reaction-diffusion systems, J. Comput. Appl. Math. 220 (2008) 215–225.

[14] R. Garrappa, The Mittag-Leffler function, `http://www.mathworks.com/matlabcentral/fileexchange/48154-the-mittag-leffler-function`, 2015.

[15] R. Garrappa, Numerical evaluation of two and three parameter Mittag-Leffler functions, SIAM J. Numer. Anal. 53 (2015) 1350–1369.

[16] R. Gorenflo, A.A. Kilbas, F. Mainardi, S.V. Rogosin, Mittag-Leffler functions, related topics and applications, Springer Monographs in Mathematics, Springer, Heidelberg, 2014.

[17] A. Hanyga, R.L. Magin, A new anisotropic fractional model of diffusion suitable for applications of diffusion tensor imaging in biological tissues, Proc. R. Soc. Lond. Ser. A Math. Phys. Eng. Sci. 470 (2014) 20140319.

[18] F. Höfling, T. Franosch, Anomalous transport in the crowded world of biological cells, Rep. Progr. Phys. 76 (2013) 046602, 50.

[19] M. Hori, I. Fukunaga, Y. Masutani, T. Taoka, K. Kamagata, Y. Suzuki, S. Aoki, Visualizing non-Gaussian diffusion: Clinical application of q-space imaging and diffusional kurtosis imaging of the brain and spine, Magn. Reson. Med. Sci. 11 (2012) 221–233.

[20] L.G. Ixaru, G. Vanden Berghe, Exponential fitting, volume 568 of *Mathematics and its Applications*, Kluwer Academic Publishers, Dordrecht, 2004.

[21] H. Jiang, F. Liu, I. Turner, K. Burrage, Analytical solutions for the multi-term time-fractional diffusion-wave/diffusion equations in a finite domain, Comput. Math. Appl. 64 (2012) 3377–3388.

[22] S.P. Kelow, K.M. Hayden, Particular solution to a time-fractional heat equation, JURP (2013).

[23] M.M. Khader, On the numerical solutions for the fractional diffusion equation, Commun. Nonlinear Sci. Numer. Simul. 16 (2011) 2535–2542.

[24] A.A. Kilbas, H.M. Srivastava, J.J. Trujillo, Theory and applications of fractional differential equations, volume 204 of *North-Holland Mathematics Studies*, Elsevier Science B.V., Amsterdam, 2006.

[25] R. Klages, G. Radons, I.M. Sokolov, Anomalous transport: foundations and applications, John Wiley & Sons, 2008.

[26] X. Li, C. Xu, Existence and uniqueness of the weak solution of the space-time fractional diffusion equation and a spectral method approximation, Commun. Comput. Phys. 8 (2010) 1016–1051.

[27] Y. Luchko, Some uniqueness and existence results for the initial-boundary-value problems for the generalized time-fractional diffusion equation, Comput. Math. Appl. 59 (2010) 1766–1772.

[28] Y. Luchko, Initial-boundary-value problems for the one-dimensional time-fractional diffusion equation, Fract. Calc. Appl. Anal. 15 (2012) 141–160.

[29] R. Magin, O. Abdullah, D. Baleanu, X. Zhou, Anomalous diffusion expressed through fractional order differential operators in the Bloch-Torrey equation, J. Magn. Reson. 190 (2008) 255–270.

[30] F. Mainardi, Fractional calculus and waves in linear viscoelasticity: an introduction to mathematical models, World Scientific, 2010.

[31] B. Mandelbrot, J. Van Ness, Fractional Brownian motions, fractional noises and applications, SIAM Rev. 10 (1968) 422–437.

[32] M.M. Meerschaert, R.L. Magin, A.Q. Ye, Anisotropic fractional diffusion tensor imaging, J. Vib. Control 22 (2016) 2211–2221.

[33] R. Metzler, J. Klafter, The random walk's guide to anomalous diffusion: a fractional dynamics approach, Phys. Rep. 339 (2000) 77.

[34] C. Necula, Option pricing in a fractional Brownian motion environment, Math. Rep. (Bucur.) 6(56) (2004) 259–273.

[35] I. Podlubny, Fractional differential equations, volume 198 of *Mathematics in Science and Engineering*, Academic Press, Inc., San Diego, CA, 1999. An introduction to fractional derivatives, fractional differential equations, to methods of their solution and some of their applications.

[36] I. Podlubny, M. Kacenak, The Matlab mlf code, MATLAB Central File Exchange (2001–2009). File ID 8738 (2001).

[37] D. Reiter, R. Magin, W. Li, J. Trujillo, M. Pilar Velasco, R. Spencer, Anomalous T2 relaxation in normal and degraded cartilage, Magn. Reson. Med. 76 (2016) 953–962.

[38] W.E. Schiesser, The numerical method of lines, Academic Press, Inc., San Diego, CA, 1991. Integration of partial differential equations.

[39] W.E. Schiesser, G.W. Griffiths, A compendium of partial differential equation models, Cambridge University Press, Cambridge, 2009. Method of lines analysis with Matlab.

[40] J. Shen, C. Li, H. Wu, M. Kalantari, Fractional order viscoelasticity in characterization for atrial tissue, Korea-Aust. Rheol. J. 25 (2013) 87–93.

[41] N. Sugimoto, Burgers equation with a fractional derivative; hereditary effects on nonlinear acoustic waves, J. Fluid Mech. 225 (1991) 631–653.

[42] P.J. Torvik, R.L. Bagley, On the appearance of the fractional derivative in the behavior of real materials, Trans. ASME J. Appl. Mech. 51 (1984) 294–298.

[43] M. Zayernouri, G.E. Karniadakis, Fractional Sturm-Liouville eigen-problems: theory and numerical approximation, J. Comput. Phys. 252 (2013) 495–517.

[44] M. Zayernouri, G.E. Karniadakis, Exponentially accurate spectral and spectral element methods for fractional ODEs, J. Comput. Phys. 257 (2014) 460–480.

[45] M. Zayernouri, G.E. Karniadakis, Fractional spectral collocation method, SIAM J. Sci. Comput. 36 (2014) A40–A62.

[46] M. Zayernouri, G.E. Karniadakis, Fractional spectral collocation methods for linear and nonlinear variable order FPDEs, J. Comput. Phys. 293 (2015) 312–338.